Title
Adipocyte HDAC4 activation leads to beige adipocyte expansion and reduced adiposity

Journal
Journal of Endocrinology, 239(2)

ISSN
0022-0795

Authors
Paulo, Esther
Wu, Dongmei
Hecker, Peter
et al.

Publication Date
2018-11-01

DOI
10.1530/joe-18-0173

Peer reviewed

HHS Public Access

Author manuscript

J Endocrinol. Author manuscript; available in PMC 2019 November 01.

Published in final edited form as:

J Endocrinol. 2018 November 01; 239(2): 153–165. doi:10.1530/JOE-18-0173.

Adipocyte HDAC4 activation leads to beige adipocyte expansion and reduced adiposity

Esther Paulo[#], **Dongmei Wu**[#], **Peter Hecker**, **Yun Zhang**, and **Biao Wang**[*]

Department of Physiology, Cardiovascular Research Institute, University of California, San Francisco, CA, USA

[#] These authors contributed equally to this work.

Abstract

Numerous studies have suggested that beige adipocyte abundance is correlated with improved metabolic performance, but direct evidence showing that beige adipocyte expansion protects animals from the development of obesity is missing. Previously, we have described that the Liver kinase b1 (Lkb1) regulates beige adipocyte renaissance in subcutaneous inguinal white adipose tissue (iWAT) through a class IIa histone deacetylase 4 (HDAC4)-dependent mechanism. This study investigates the physiological impact of persistent beige adipocyte renaissance in energy homeostasis in mice. Here we present that the transgenic mice H4-TG, overexpressing constitutively active HDAC4 in adipocytes, showed beige adipocyte expansion in iWAT at room temperature. H4-TG mice exhibited increased energy expenditure due to beige adipocyte expansion. They also exhibited reduced adiposity under both normal chow and high-fat diet (HFD) feeding conditions. Specific ablation of beige adipocytes reversed the protection against HFD-induced obesity in H4-TG mice. Taken together, our results directly demonstrate that beige adipocyte expansion regulates adiposity in mice, and targeting beige adipocyte renaissance may present a novel strategy to tackle obesity in humans.

Keywords

Beige adipocytes; Adaptive thermogenesis; obesity; HDAC4; cell ablation

Introduction

Two types of UCP1$^+$ adipocytes have been characterized by their differences in anatomic localization, developmental origin, and molecular signature in rodents (Harms and Seale, 2013; Kajimura et al., 2015). The classical brown adipocytes are present in interscapular and perirenal adipose tissues, and they originate from Myf5$^+$/Pax7$^+$ skeletal muscle progenitors (Seale et al., 2008). The beige adipocytes are formed and clustered within the subcutaneous inguinal white adipose tissue (iWAT) in response to β-adrenergic receptor (βAR) stimulation

[*]Corresponding Author, Biao Wang Ph.D., 555 Mission Bay Blvd South, Room 252Y, San Francisco, CA 94158, Phone: 415-502-2023, biao.wang@ucsf.edu.

Author contributions:B.W., E.P. and D.W. planned the experiments and wrote the manuscript. D.W. characterized H4-TG mice phenotype and E.P. performed beige adipocyte ablation studies. P.H analyzed microarray data. Y.Z. assisted with mouse genotyping.

Declaration of interest: Authors declare no conflict of interest.

(Cohen et al., 2014; Seale et al., 2011; Walden et al., 2012; Wu et al., 2012). Beige adipocytes are either derived from mural progenitors that reside in iWAT (Berry et al., 2016; Lee et al., 2012; Vishvanath et al., 2015; Wu et al., 2012), or they may arise from transdifferentiation of white adipocytes (Barbatelli et al., 2010; Cinti, 2009; Rosenwald et al., 2013).

Several studies using anatomical and gene profiling approaches have indicated that interscapular brown fat from human infants and neck brown fat from human adults shares features with classical murine brown adipocytes, while supraclavicular fat of adult humans mainly consists of beige adipocytes (Cypess et al., 2015; Cypess et al., 2013; Jespersen et al., 2013; Lee et al., 2014; Lidell et al., 2013; Sharp et al., 2012). However, specific functions of beige adipocytes have not been addressed for two major reasons. Beige adipocytes tend to be activated together with brown adipocytes in response to the same stimuli, and the tools currently used for genetic manipulations in mice cannot distinguish between these two cell types.

The beige adipocytes formed postnatally in iWAT can lose thermogenic gene expression and multilocular morphology at the adult stage, but βAR stimuli can restore their “beigeing” properties, a phenomenon termed as “beige adipocyte renaissance” (Lee et al., 2015; Wang et al., 2017). We have demonstrated that beige adipocyte renaissance is governed by cyclic adenosine 3’,5’-monophosphate (cAMP) and histone deacetylase 4 (HDAC4) signaling in white adipocytes (Wang et al., 2017). We have shown that HDAC4 is activated in adipocytes of both iWAT and interscapular brown adipose tissue (iBAT) from pan adipocyte-specific Liver kinase b1 (Lkb1) knockout mice (the $Lkb1^{AKO}$ mice), but its activation is necessary for beige adipocyte renaissance in iWAT. The mice expressing constitutively active HDAC4 in adipocytes (H4-TG) exhibit persistent beige adipocyte renaissance in iWAT without affecting thermogenic capacity in iBAT, and improved metabolic performance under both normal chow and high-fat diet conditions. Ablating beige adipocytes in H4-TG mice abolished the protective effects on HFD-induced obesity, suggesting that beige adipocytes can regulate adiposity.

Materials and Methods

Mice:

All animal experiments were approved by the UCSF IACUC Committee in adherence to NIH guidelines and policies. Rosa-iDTR (JAX#007900) mice were obtained from JAX. Ucp1-Cre (JAX#024670) mice were provided by Dr. Evan Rosen. A 5.6kb fragment of the ap2 promoter (provided by Dr. Ronald Evans) and a 4kb fragment encoding GFP-HDAC4.S245/467/632A (mutation of the three Salt-inducible kinase phosphorylation sites to alanine) were used to generate the ap2-GFP-HDAC4.3A transgenic mouse. The transgenic mice (line C and D) had been backcrossed into C57bl/6J background for more than 5 generations before metabolic analysis. Both male and female mice were used for thermogenic studies. Male mice were used in metabolic studies because they were more prone to high-fat diet induced obesity and other metabolic abnormalities (Yang et al., 2014). Mice were housed in a temperature-controlled environment at 22ºC under a 12h light:dark cycle with free access to water and food (PicoLab® Rodent Diet 20, #5053). For

thermoneutral housing, ~4-week-old mice were placed in a 30°C rodent chamber (Power Scientific RIS52SD Rodent Incubator) for additional 4 weeks.

Browning of white adipose tissue:

For cold stimulation experiments, mice were placed in an 8°C rodent chamber (Power Scientific RIS52SD Rodent Incubator) for 7 days. For CL 316,243 (CL) treatment, mice were injected intraperitoneally with 1 mg g^{-1} daily for 7 days. To identify beige adipocytes, subcutaneous inguinal fat (iWAT) was isolated and Ucp1 RNA and protein levels were analyzed. Paraffin sections and hematoxylin & eosin (H&E) staining were performed at AML Labs using standard protocols.

Beige adipocyte ablation:

Three week-old male mice were injected with a single diphtheria toxin (DT) intraperitoneally at the dose of 10–25 ng/mouse (Biological Laboratories Inc.).

Metabolic measurements:

Total energy expenditure (TEE) and respiratory exchange ratio (RER) were measured using CLAMS (Columbus Instruments), installed under a constant temperature-controlled environment, under a 12 hour light: dark cycle with free access to food and water. To determine βAR-induced TEE, CL (1 mg g^{-1}) was injected intraperitoneally at ~10am of the last day of CLAMS run. The raw data were normalized per mouse (Butler and Kozak, 2010; Tschop et al., 2012). The energy expenditure of physical activity (PAEE) and the thermogenic effect of food (TEF) were calculated as described before (Abreu-Vieira et al., 2015). Magnetic resonance imaging scans for fat and lean mass were performed using an Echo MRI-100 instrument according to manufacturer's instructions. Investigators were blinded to mice genotypes for CLAMS, which were performed by the UCSF Diabetes and Endocrinology Research Center Metabolic Research Unit. For high fat diet (HFD) studies, 6-week-old male mice were transferred to a 60% fat diet (Research Diets, D12492) at room temperature. Body weight was monitored weekly. For insulin tolerance test (ITT), mice were fasted 4–6h before intraperitoneal administration of insulin (Humulin; 0.75U kg^{-1}). Serum glucose was measured from tail vein at indicated time points with a glucometer (Contour, Bayer). Serum TAG levels were measured using Infinity Triglycerides Reagent kit (Thermo Scientific), and serum insulin levels were determined using Mouse insulin ultrasensitive ELISA kit (Alpco).

Histology:

Tissues were fixed in 10% formalin, and processed and stained at AML Laboratories. Cell size was measured using ImageJ. Adipocyte size distribution was calculated using total adipocyte numbers counted in different areas from multiple sections.

Cold tolerance test (CTT):

6–8-week-old male and female mice were single-housed with free-access to food and water during CTT. Rectal temperature was monitored hourly during 4°C cold challenge with a

BAT-12 Microprobe Thermometer (Physitem Instruments). Cold challenge was started at 11am (4 hours after light on).

Tissue catecholamine measurement:

Catecholamines levels were measured by ELISA (Rocky Mountain Diagnostics, # BA E-6600) according to the manufacturer's protocol. Tissues were homogenized in homogenization buffer (0.01N HCl, 1 mM EDTA, 4 mM $Na_2S_2O_5$), and centrifuged at 13,000 rpm for 15 min at 4°C. The supernatants were collected and stored at −80°C prior to quantification. All measurements were normalized to total tissue protein concentration.

Respiration *ex vivo*:

For measurements of tissue respiration activity *ex vivo*, the minced inguinal fat tissues were added in the chamber that contained prewarmed respiration buffer at 37°C. Then the tissue oxygen consumption rates were measured using a Clarke electrode (Strathkelvin Instruments) using the established protocol (Li and Graham, 2012). Oxygen consumption was normalized to tissue weight.

RNA analysis:

RNA from cells and tissues was extracted using RNeasy Mini Kit (QIAGEN). Total RNA (1 μg) was reverse-transcribed by iScript™ cDNA synthesis kit (Bio-Rad) and cDNA was used for real time PT-PCR (CFX384, Bio-Rad), using 2 ng of cDNA template and a primer concentration of 400 nM. Values were normalized to 36b4 housekeeping gene. Primer sequences were listed in Supplementary table 1. Pooled cDNA from iWAT of ~ 8-week-old male WT and H4-TG mice were used for Affymetrix Mouse Gene Array 1.0 using the protocol provided by manufacturer. The data was deposited in NCBI GEO (# GSE106310). Gene-ontology analysis was performed using Metascape at http://metascrape.org.

Western blot:

Tissues were homogenized on ice in lysis-buffer (50 mM Tris-HCl, 150 mM NaCl, 1 mM EDTA, 6 mM EGTA, 20 mM NaF, 1% Triton X-100, and protease inhibitors) for 15–20 min. After centrifugation at 13000 rpm for 15 min, supernatants were reserved for protein quantification followed by SDS-PAGE analysis. The following antibodies were used: anti-Hdac4 (Cell Signaling Technology, #7628), anti-Hsp90 (Santa Cruz Biotechnology, #SC-7947), and anti-Ucp1 (Sigma, #U6382).

Statistical analysis:

We used GraphPad Prism 6.0 to assess data for normal distribution and similar variance between groups. Data were presented as the mean ± s.d. Statistical significance was determined using an unpaired two-tailed Student's *t* test with unequal variance between groups: ns: not significant, *: $p<0.05$ and **: $p<0.01$. We selected sample size for animal experiments based on numbers typically used in similar published studies. We did not perform randomization of animals or predetermine sample size by a statistical method.

Results

Mice expressing constitutively active HDAC4 exhibit beige adipocyte expansion in iWAT

We have employed pan adipocyte-specific Adiponectin-Cre and brown/beige adipocyte-specific Ucp1-Cre to investigate roles of liver kinase b1 (Lkb1) in adipocytes to demonstrate that Lkb1 regulates two distinct pathways in brown and beige adipocytes. In brown adipocytes, Lkb1 appears to govern thermogenic capacity independently of HDAC4 (Masand et al., 2018); but in white adipocytes, it controls HDAC4 activity (through Salt-inducible kinases/SIKs) to regulate beige adipocyte renaissance non-cell autonomously (Wang et al., 2017). We reasoned that HDAC4 activation in white adipocytes could promote beige adipocyte renaissance in iWAT without affecting adaptive thermogenesis in BAT, and this unique requirement of HDAC4 for beige adipocyte renaissance could enable us to address beige adipocyte specific function in energy homeostasis. In this report, we have generated a transgenic mouse line, expressing constitutively active HDAC4 (GFP-HDAC4.3A with all SIKs phosphorylation sites mutated to alanine) under the control of an ap2 promoter (Fig. 1A, top). The transgene was expressed in both white and brown adipose tissues, but not in muscle and liver in two separate lines (line C and line D) (Fig. 1A, bottom, Supplemental Fig. 3A). The line D (referred as H4-TG#D throughout this study) was selected for further detailed characterizations. Immunoblots further confirmed that the transgene GFP-HDAC4.3A was over-expressed in mature adipocytes, not in stromal vascular fraction (SVF) cells (Supplemental Fig. 1A). The male H4-TG#D mice had similar *Ucp1* expression and multilocular brown adipocyte morphology, and they were similarly cold resistant as wild-type mice at ~8-week of age (Supplementary Fig. 1B-E). In contrast, we have observed increased *Ucp1* mRNA levels in iWAT from these H4-TG#D male mice at 8-week of age, although there were no detectable differences in *Ucp1* transcript levels at 3-week of age (Fig. 1B). Histological analysis (H&E staining) also confirmed the presence of multilocular beige adipocyte expansion in iWAT of adult H4-TG#D mice (Fig. 1C), which resembled the beige adipocyte expansion phenotype observed in $Lkb1^{AKO}$ mice (Wang et al., 2017). Gender did not affect beige adipocyte expansion caused by constitutively HDAC4 action, because elevated thermogenic gene expression and multilocular morphology were also observed in the iWAT of female H4-TG#D mice at ~8-week of age (Supplementary Fig. 2A-B). Beige adipocyte presence in H4-TG#D mice also required sympathetic inputs, as thermoneutral housing reduced Ucp1 mRNA and protein levels in iWAT of H4-TG mice (Fig. 1B, Supplementary Fig. 6A). On the other hand, CL316243 (a β3 specific agonist, abbreviated as CL) administration did not further induce Ucp1 protein levels in adult H4-TG#D mice (Fig. 1D). Notably, the H4-TG#C mice also exhibited elevated thermogenic gene expression and Ucp1 protein levels in iWAT (Supplementary Fig. 3B-C).

We have described that adipocyte Lkb1 deficiency led to Hdac4 activation in adipocytes, which promoted beige adipocyte renaissance in iWAT (Fig. 2A) (Wang et al., 2017). The gene profiling study revealed that there were over 500 genes were upregulated in iWAT by Lkb1 deficiency in white adipocytes. We then performed microarray experiment in the H4-TG#D mice and compared the transcriptomic changes in the iWAT caused by adipocyte Lkb1 deficiency (in $Lkb1^{AKO}$ mice) and constitutively active HDAC4 overexpression (in H4-TG mice). In fact, about half of genes upregulated in the iWAT of $Lkb1^{AKO}$ mice were

also upregulated in H4-TG#D mice (Fig. 2B). Detailed gene-ontology (GO) analysis on these shared regulated genes suggested that the top four enriched GO terms were related to muscle and metabolic functions (Fig. 2C), consistent with the histological observation of the expansion of thermogenic active beige adipocytes in iWAT. The qPCR analysis further confirmed that many thermogenic signature genes and metabolic genes were upregulated in iWAT of H4-TG#D mice (Fig. 2D). Collectively, adipocyte HDAC4 activation is necessary and sufficient to promote beige adipocyte expansion in iWAT of adult mice. The ap2 promoter was not exclusively active in adipocytes (Lee et al., 2013; Mullican et al., 2013). The sympathetic activity mainly regulates the catecholamine turnover of in the iWAT, and the issue catecholamine levels were not affected (WT 18.8 vs H4-TG 16.2 pg/g protein). The contribution of macrophage to catecholamine secretion is under debate (Fischer et al., 2017; Qiu et al., 2014; Reitman, 2017). Inflammation and macrophage marker genes were not altered in iWAT of H4-TG#D mice (Supplementary Fig. 4A), suggesting that catecholamines produced in immune cells is unlikely causing the beige adipocyte expansion in H4-TG#D mice. However, we cannot fully rule out the possibility that HDAC4 in other cell types may lead to the beige adipocyte expansion in iWAT.

Previously, we have characterized an Ucp1-Cre inducible diphtheria toxin receptor (iDTR) mediated cell ablation system (the Ucp1-Cre;ROSA-iDTR mice), where beige adipocytes can be permanently ablated in iWAT upon diphtheria toxin (DT) injection (Fig. 3A) (Wang et al., 2017). We then generated H4-TG#D;Ucp1-Cre;Rosa-iDTR (abbreviated as H4-TG#D;Cre+) mice. DT injection at 3-week of age ablated beige adipocytes in H4-TG#D;Cre + mice (Fig. 3B-C). In these mice, CL was unable to induce *Ucp1* expression anymore at adult stage (Fig. 3D). Thus, overexpression of constitutively active GFP-HDAC4.3A was not sufficient to convert white adipocytes to beige adipocytes cell-autonomously in beige adipocyte-ablated H4-TG#D;Cre+ mice. Instead, HDAC4 activation in white adipocytes maintained beigeing properties of preexisting beige adipocytes in iWAT, suggesting that beige adipocyte expansion in H4-TG#D mice was formed through the same persistent "renaissance" mechanism observed in the $Lkb1^{AKO}$ mice.

H4-TG mice show increased energy expenditure

Beige adipocytes are capable of Ucp1-dependent and –independent thermogenesis (Ikeda et al., 2017; Kazak et al., 2015; Shabalina et al., 2013). We then measured whether beige adipocyte expansion in iWAT contributed to total energy expenditure (TEE) at room temperature. Indeed, there was about 50% increase of thermogenic capacity of iWAT from H4-TG#D mice *ex vivo* (Supplementary Fig. 4B). Indirect calorimetry experiments showed that 8week-old H4-TG#D male mice exhibited increased basal TEE particularly at night (Fig 4.A), although CL-induced EE was not affected (Supplementary Fig. 5). Scatter plots confirmed that elevated TEE in H4-TG#D mice was independent of body weight (Fig 4.B). Respiratory exchange ratio (RER) was not altered (Fig. 4C). Food intake and physical activities were slightly increased (Fig. 4 D-E), Regarding the partitioning of TEE, the percentage of energy expenditure of physical activity (%PAEE) was increased from 14% to 20% at night, but that of thermogenic effect of food (%TEF) was not altered in the H4-TG#D mice (Fig. 4F).

The contribution of adaptive thermogenesis to total energy expenditure is dependent on ambient temperature (Abreu-Vieira et al., 2015; Cannon and Nedergaard, 2011; Ganeshan and Chawla, 2017; Maloney et al., 2014). We next determined whether the absence of thermogenic active beige adipocytes in H4-TG#D mice at thermoneutrality would affect energy expenditure. At thermoneutrality, Ucp1 mRNA and protein levels were decreased, and brown adipocytes exhibited unilocular morphology in both WT and H4-TG#D mice (Supplementary Fig. 6A-C). Elevated Ucp1 expression in the iWAT was also abolished in H4-TG#D mice (Fig. 1B, Supplementary Fig. 6A). Basal TEE at night in H4-TG#D mice was not increased (Supplementary Fig. 6D-E). RER and food intake were not different (Supplementary Fig. 6F-G). Physical activity in H4-TG#D mice remained elevated at thermoneutrality, although the %PAEE was no longer elevated (Supplementary Fig. 6H-I). These data suggest that expanded beige adipocytes in iWAT and increased physical activity contributed to increased basal TEE in H4-TG#D mice at room temperature.

H4-TG mice show improved metabolic performance

Thus, we employed H4-TG#D mice as a model system to study metabolic consequences of beige adipocyte expansion. Under normal chow feeding, H4-TG#D mice had reduced body weight in an age-dependent manner (Fig. 5A). At ~6-month of age, the reduced body weight in H4-TG#D mice was due to reduced fat mass, but not lean mass (Fig. 5B-C). Food intake was also increased at night (Fig. 5D), possibly secondary to reduced obesity. H4-TG#D mice had smaller adipocytes (measured by histological analysis on H&E sections) and less macrophage infiltration (determined by q-PCR analysis of *Cd68* and *F4/80*) in epididymal WAT (eWAT) (Fig. 5E-G). Serum triglyceride, insulin and glucose levels were all reduced in these mice (Fig. 5H-J), suggesting that H4-TG#D mice showed reduced adiposity and improved glucose and lipid metabolism.

We have demonstrated that the persistent beige adipocyte population in $Lkb1^{AKO}$ mice is sustained during HFD-induced obesity (Wang et al., 2017). Since H4-TG mice and $Lkb1^{AKO}$ mice exhibited beige adipocyte expansion in iWAT through the same "renaissance" mechanism, we also analyzed whether H4-TG#D male mice could also maintain beige adipocyte expansion even after HFD. Histological analysis confirmed the presence of multilocular beige adipocytes in the iWAT after 4–5 weeks HFD (Supplementary Fig. 7B). Immunblot analysis also showed that Ucp1 protein levels remained elevated (Supplementary Fig. 7A). Additional beige adipocyte markers that were upregulated in H4-TG#D mice at normal chow also remained elevated after 4-week HFD (Fig. 2D, Supplementary Fig. 9A).

Then we investigated whether H4-TG#D mice were also protected against HFD-induced metabolic abnormalities. Indeed, H4-TG#D mice showed reduced body weight on HFD (as early as in 2 weeks), and the difference in weight gain between H4-TG and control mice became greater with longer HFD feeding (Fig. 6A). The reduced body weight under HFD was also observed in the H4-TG#C mice (Supplemental Fig. 8). The reduced body weight in H4-TG#D mice under HFD was only contributed by reduced fat mass, while the lean mass was not affected (Fig. 6B-C). Food intake was slightly upregulated at day in H4-TG#D mice (Fig. 6D). Histological analysis showed the reduced adipocyte size in the eWAT of H4-

TG#D mice (Fig. 6E-F). The reduced adiposity under HFD (and NC) was not due to defects in adipogenesis, because mRNA levels of adipogenesis markers were not reduced in the eWAT of H4-TG#D mice (Supplementary Fig. 10A-B). Notably, there were less crown-like structures in the eWAT of H4-TG#D mice after HFD (Fig. 6E). Additional qPCR analysis of macrophage markers confirmed that adipose inflammation was reduced in H4-TG#D mice (Fig. 6G). Furthermore, H4-TG#D mice were more insulin sensitive; they showed enhanced glucose clearance in ITT (Fig. 6H-I). Collectively, H4-TG#D mice displayed metabolic improvements, such as reduced adiposity and enhanced insulin sensitivity, under normal chow and HFD.

Beige adipocyte ablation in H4-TG mice reverses protection against HFD-induced obesity

In order to determine whether thermogenic activity of beige adipocytes in H4-TG contributed to the metabolic phenotypes, we generated H4-TG mice in Ucp1 KO background (referred as H4-TG;Ucp1 KO mice). There was an expansion of multilocular beige-like adipocytes in iWAT of Ucp1 KO mice, as previously reported (Enerback et al., 1997; Liu et al., 2003). These multilocular but Ucp1^{-} adipocytes remained in iWAT of H4-TG;Ucp1 KO mice (Supplementary Fig.11B). The q-PCR analysis showed thermogenic gene program in iWAT from H4-TG;Ucp1 KO mice was further induced compared to that of H4-TG or Ucp1 KO mice alone (Supplementary Fig.11A). Under HFD, H4-TG;Ucp1 KO mice exhibited further reduced body weight, although there was no significant body weight difference between WT and Ucp1 KO mice during 4-week HFD (Supplementary Fig.11C). These observations suggest that enhanced Ucp1-dependent thermogenic activity from expanded beige adipocytes in H4-TG mice does not contribute to their metabolic phenotypes under HFD. But the caveat of this approach is that Ucp1 deficiency alone can induce compensatory thermogenic mechanisms that ultimately affect systemic insulin sensitivity (Ikeda et al., 2017; Kazak et al., 2015).

Then we used the beige adipocyte ablation approach described earlier to investigate whether beige adipocytes can regulate metabolic behavior (Fig. 3A). We generated four groups of mice: Cre- (genotype: *Rosa-iDTR*), Cre+ (genotype: *Ucp1-Cre; Rosa-iDTR*), H4-TG#D;Cre- (genotype: *H4-TG#D;Rosa-iDTR*), and H4-TG#D;Cre+ (genotype: *H4-TG#D;Ucp1-Cre;Rosa-iDTR*) (Fig. 7A). The postnatal beige adipocytes were ablated in the Cre+ and H4-TG#D;Cre+ after DT injection at three-week of age, and they remained absent for two months (Fig. 7B-D). While DT injection did not affect beige adipocyte abundance in the H4-TG#D;Cre- mice (Fig. 7D). Importantly, beige adipocyte ablation in H4-TG#D;Cre+ mice did not affect *Ucp1* mRNA levels, multilocular morphology in iBAT and cold resistance in 4°C cold test (Supplementary Fig.12A-C). We then determined metabolic behaviors of beige adipocyte-ablated H4-TG#D mice under HFD (Fig. 7B). Beige adipocyte-ablated H4-TG#D (H4-TG#D;Cre+) mice gained more weight compared with H4-TG#D mice without beige ablation (H4-TG#D;Cre-) during initial weeks of HFD (Fig. 7E-F). This effect was not due to alteration of adipocyte numbers in adipose tissues by DT-mediated cell ablation, as beige ablation in wild-type mice had no effect. However, H4-TG#D;Cre+ mice remained improved insulin sensitivity compared with H4-TG#D;Cre- mice (Fig. 7G-H), suggesting that HDAC4 activation in white adipocytes in H4-TG mice might regulate insulin sensitivity independently of beige adipocyte expansion. Thus, changes of

ITT are not simply a consequence of reduced adiposity in the H4-TG#D mice. These observations also suggest that beige adipocytes in H4-TG#D mice specifically regulate adiposity under an obesogenic diet presumably through an Ucp1-dependent mechanism.

Discussion

Numerous studies have observed that beige adipocyte expansion correlated with improved metabolic performance in rodents and humans; however, the casualty between them has not been established. This is partially due to a conundrum facing the adipocyte research community that no perfect Cre lines are available to target white, beige or brown adipocyte specifically. Previously, we have used both Adiponectin-Cre and Ucp1-Cre to generate pan adipocyte-specific and brown/beige adipocyte-specific Lkb1 knockout mice ($Lkb1^{AKO}$ and $Lkb1^{BKO}$ mice respectively), and identified that Lkb1-SIKs-HDAC4 pathway in white adipocytes regulated beige adipocyte maintenance in iWAT in a non-cell autonomous fashion, a process called beige adipocyte renaissance (Wang et al., 2017). In fact, Lkb1 deficiency in beige adipocytes themselves did not affect beige adipocyte dynamics in iWAT. Hence, the beige adipocyte expansion phenotype in many Adiponectin promoter-driven overexpression or knockout mouse models should be interpreted with caution. Combinational studies using Adiponectin-Cre and Ucp1-Cre are needed to determine whether the pathways of interest regulate beige adipocyte formation cell autonomously or non-cell autonomously.

It has been demonstrated that beige adipocytes may have additional roles in energy metabolism rather than Ucp1-dependent and –independent adaptive thermogenesis (Ikeda et al., 2017; Kajimura et al., 2015; Kazak et al., 2015). However, experimental evidence definitely showing specific functions of beige adipocytes is still lacking. One possible route to address beige adipocyte-specific function is to identify genetic programs that only affect beige adipocytes. We showed that HDAC4 activation by Lkb1 deficiency was specifically required for beige adipocyte renaissance in iWAT, and it did not regulate adaptive thermogenesis in brown adipocytes (Paulo et al., 2018; Wang et al., 2017). On the other hand, HDAC4 loss-of-function did not affect adaptive thermogenesis in brown adipocytes in either wild-type mice or in adipocyte Lkb1 deficiency background (Wang et al., 2017). Consistent with our previous report, constitutively active HDAC4 overexpression in adipocytes drives the persistent beige adipocyte renaissance in iWAT, similar to HDAC4 overactivation caused by Lkb1 deficiency in adipocytes. This specific requirement of HDAC4 in beige adipocyte expansion enabled us to explore beige adipocyte-specific function in energy homeostasis using the H4-TG mice. In combination with a novel beige adipocyte ablation system (Wang et al., 2017), we showed that specific ablation of $Ucp1^{+}$ beige adipocytes did reverse protection against HDF-induced obesity in H4-TG mice, establishing a causal link between beige adipocyte abundance and adiposity. Furthermore, this novel beige adipocyte ablation approach will be also applicable to address numerous aspects of beige adipocyte biology.

There are some caveats in the current study. The promiscuous ap2 promoter used in H4-TG mice could overexpress constitutively active HDAC4 in non-adipocyte cells including adipogenic progenitors, neurons, macrophages and endothelial cells (Jeffery et al., 2014; Lee

et al., 2013; Mullican et al., 2013; Shan et al., 2013). These potential off-target effects of constitutively active HDAC4 might indirectly contribute to beige adipocyte expansion in iWAT and improved metabolic performance, such as improved insulin sensitivity and elevated physical activity. Additional studies using Adiponectin promoter-driven conditional (spatial and/or temporal) overexpression of constitutively active HDAC4 will address this concern.

Although expanded beige adipocytes in both Lkb1^{AKO} and H4-TG mice were present during short-term HFD (~4 weeks), they did lose their beigeing properties after long-term HFD (~10 weeks) (Supplementary Fig.9A-B) (Wang et al., 2017). Therefore, we only performed 4–5 week HDF experiments in H4-TG mice after beige adipocyte ablation, to establish the causality relationship between beige adipocyte abundance and reduced adiposity. Whether the presence of beige adipocytes during early-phase HFD contributes to metabolic improvements in H4-TG mice after long-term HFD remains unknown. Regardless, our study provides direct evidence that beige adipocytes could regulate adiposity. Future studies are warranted to use these animal models to investigate whether thermogenic or non-thermogenic function of beige adipocytes is required for the anti-obesity effect in H4-TG mice.

Supplementary Material

Refer to Web version on PubMed Central for supplementary material.

Acknowledgements:

We thank X-J. Yang (McGill University) for providing the GFP-HDAC4.3A plasmid. We thank C. Paillart for assistance with CLAMS experiments and L. Ouyang (The Salk Institute for Biological Studies) for microarray experiment.

Funding:

This work is supported by National Institutes of Health (NIH) grants DK105175, UCSF Diabetes Research Center P30DK063720, UCSF Nutrition Obesity Research Center P30DK098722, and research grants from Hillblom Foundation and Juvenile Diabetes Research Foundation (B.W.). E.P. is supported by a fellowship grant from Hillblom Foundation.

References:

Abreu-Vieira G, Xiao C, Gavrilova O, and Reitman ML (2015). Integration of body temperature into the analysis of energy expenditure in the mouse. Molecular metabolism 4, 461–470. [PubMed: 26042200]

Barbatelli G, Murano I, Madsen L, Hao Q, Jimenez M, Kristiansen K, Giacobino JP, De Matteis R, and Cinti S (2010). The emergence of cold-induced brown adipocytes in mouse white fat depots is determined predominantly by white to brown adipocyte transdifferentiation. American journal of physiology Endocrinology and metabolism 298, E1244–1253. [PubMed: 20354155]

Berry DC, Jiang Y, and Graff JM (2016). Mouse strains to study cold-inducible beige progenitors and beige adipocyte formation and function. Nature communications 7, 10184.

Butler AA, and Kozak LP (2010). A recurring problem with the analysis of energy expenditure in genetic models expressing lean and obese phenotypes. Diabetes 59, 323–329. [PubMed: 20103710]

Cannon B, and Nedergaard J. (2011). Nonshivering thermogenesis and its adequate measurement in metabolic studies. The Journal of experimental biology 214, 242–253. [PubMed: 21177944]

Cinti S (2009). Reversible physiological transdifferentiation in the adipose organ. The Proceedings of the Nutrition Society 68, 340–349. [PubMed: 19698198]

Cohen P, Levy JD, Zhang Y, Frontini A, Kolodin DP, Svensson KJ, Lo JC, Zeng X, Ye L, Khandekar MJ, et al. (2014). Ablation of PRDM16 and beige adipose causes metabolic dysfunction and a subcutaneous to visceral fat switch. Cell 156, 304–316. [PubMed: 24439384]

Cypess AM, Weiner LS, Roberts-Toler C, Franquet Elia E, Kessler SH, Kahn PA, English J, Chatman K, Trauger SA, Doria A, et al. (2015). Activation of human brown adipose tissue by a beta3-adrenergic receptor agonist. Cell metabolism 21, 33–38. [PubMed: 25565203]

Cypess AM, White AP, Vernochet C, Schulz TJ, Xue R, Sass CA, Huang TL, Roberts-Toler C, Weiner LS, Sze C, et al. (2013). Anatomical localization, gene expression profiling and functional characterization of adult human neck brown fat. Nature medicine 19, 635–639.

Enerback S, Jacobsson A, Simpson EM, Guerra C, Yamashita H, Harper ME, and Kozak LP (1997). Mice lacking mitochondrial uncoupling protein are cold-sensitive but not obese. Nature 387, 90–94.

Fischer K, Ruiz HH, Jhun K, Finan B, Oberlin DJ, van der Heide V, Kalinovich AV, Petrovic N, Wolf Y, Clemmensen C, et al. (2017). Alternatively activated macrophages do not synthesize catecholamines or contribute to adipose tissue adaptive thermogenesis. Nature medicine 23, 623–630.

Ganeshan K, and Chawla A (2017). Warming the mouse to model human diseases. Nature reviews Endocrinology.

Harms M, and Seale P (2013). Brown and beige fat: development, function and therapeutic potential. Nature medicine 19, 1252–1263.

Ikeda K, Kang Q, Yoneshiro T, Camporez JP, Maki H, Homma M, Shinoda K, Chen Y, Lu X, Maretich P, et al. (2017). UCP1-independent signaling involving SERCA2b-mediated calcium cycling regulates beige fat thermogenesis and systemic glucose homeostasis. Nature medicine 23, 1454–1465.

Jeffery E, Berry R, Church CD, Yu S, Shook BA, Horsley V, Rosen ED, and Rodeheffer MS (2014). Characterization of Cre recombinase models for the study of adipose tissue. Adipocyte 3, 206–211. [PubMed: 25068087]

Jespersen NZ, Larsen TJ, Peijs L, Daugaard S, Homoe P, Loft A, de Jong J, Mathur N, Cannon B, Nedergaard J, et al. (2013). A classical brown adipose tissue mRNA signature partly overlaps with brite in the supraclavicular region of adult humans. Cell metabolism 17, 798–805. [PubMed: 23663743]

Kajimura S, Spiegelman BM, and Seale P (2015). Brown and Beige Fat: Physiological Roles beyond Heat Generation. Cell metabolism 22, 546–559. [PubMed: 26445512]

Kazak L, Chouchani ET, Jedrychowski MP, Erickson BK, Shinoda K, Cohen P, Vetrivelan R, Lu GZ, Laznik-Bogoslavski D, Hasenfuss SC, et al. (2015). A creatine-driven substrate cycle enhances energy expenditure and thermogenesis in beige fat. Cell 163, 643–655. [PubMed: 26496606]

Lee KY, Russell SJ, Ussar S, Boucher J, Vernochet C, Mori MA, Smyth G, Rourk M, Cederquist C, Rosen ED, et al. (2013). Lessons on conditional gene targeting in mouse adipose tissue. Diabetes 62, 864–874. [PubMed: 23321074]

Lee P, Werner CD, Kebebew E, and Celi FS (2014). Functional thermogenic beige adipogenesis is inducible in human neck fat. International journal of obesity 38, 170–176. [PubMed: 23736373]

Lee YH, Petkova AP, Konkar AA, and Granneman JG (2015). Cellular origins of cold-induced brown adipocytes in adult mice. FASEB journal : official publication of the Federation of American Societies for Experimental Biology 29, 286–299. [PubMed: 25392270]

Lee YH, Petkova AP, Mottillo EP, and Granneman JG (2012). In vivo identification of bipotential adipocyte progenitors recruited by beta3-adrenoceptor activation and high-fat feeding. Cell metabolism 15, 480–491. [PubMed: 22482730]

Li Z, and Graham BH (2012). Measurement of mitochondrial oxygen consumption using a Clark electrode. Methods in molecular biology 837, 63–72. [PubMed: 22215541]

Lidell ME, Betz MJ, Dahlqvist Leinhard O, Heglind M, Elander L, Slawik M, Mussack T, Nilsson D, Romu T, Nuutila P, et al. (2013). Evidence for two types of brown adipose tissue in humans. Nature medicine 19, 631–634.

Liu X, Rossmeisl M, McClaine J, Riachi M, Harper ME, and Kozak LP (2003). Paradoxical resistance to diet-induced obesity in UCP1-deficient mice. The Journal of clinical investigation 111, 399–407. [PubMed: 12569166]

Maloney SK, Fuller A, Mitchell D, Gordon C, and Overton JM (2014). Translating animal model research: does it matter that our rodents are cold? Physiology (Bethesda, Md) 29, 413–420.

Masand R, Paulo E, Wu D, Wang Y, Swaney DL, Jimenez-Morales D, Krogan NJ, and Wang B (2018). Proteome Imbalance of Mitochondrial Electron Transport Chain in Brown Adipocytes Leads to Metabolic Benefits. Cell metabolism 27, 616–629.e614. [PubMed: 29514069]

Mullican SE, Tomaru T, Gaddis CA, Peed LC, Sundaram A, and Lazar MA (2013). A novel adipose-specific gene deletion model demonstrates potential pitfalls of existing methods. Molecular endocrinology 27, 127–134. [PubMed: 23192980]

Paulo E, Wu D, Wang Y, Zhang Y, Wu Y, Swaney DL, Soucheray M, Jimenez-Morales D, Chawla A, Krogan NJ, et al. (2018). Sympathetic inputs regulate adaptive thermogenesis in brown adipose tissue through cAMP-Salt inducible kinase axis. Scientific reports 8, 11001. [PubMed: 30030465]

Qiu Y, Nguyen KD, Odegaard JI, Cui X, Tian X, Locksley RM, Palmiter RD, and Chawla A (2014). Eosinophils and type 2 cytokine signaling in macrophages orchestrate development of functional beige fat. Cell 157, 1292–1308. [PubMed: 24906148]

Reitman ML (2017). How Does Fat Transition from White to Beige? Cell metabolism 26, 14–16. [PubMed: 28683281]

Rosenwald M, Perdikari A, Rulicke T, and Wolfrum C (2013). Bi-directional interconversion of brite and white adipocytes. Nature cell biology 15, 659–667. [PubMed: 23624403]

Seale P, Bjork B, Yang W, Kajimura S, Chin S, Kuang S, Scime A, Devarakonda S, Conroe HM, Erdjument-Bromage H, et al. (2008). PRDM16 controls a brown fat/skeletal muscle switch. Nature 454, 961–967. [PubMed: 18719582]

Seale P, Conroe HM, Estall J, Kajimura S, Frontini A, Ishibashi J, Cohen P, Cinti S, and Spiegelman BM (2011). Prdm16 determines the thermogenic program of subcutaneous white adipose tissue in mice. The Journal of clinical investigation 121, 96–105. [PubMed: 21123942]

Shabalina IG, Petrovic N, de Jong JM, Kalinovich AV, Cannon B, and Nedergaard J (2013). UCP1 in brite/beige adipose tissue mitochondria is functionally thermogenic. Cell reports 5, 1196–1203.

Shan T, Liu W, and Kuang S (2013). Fatty acid binding protein 4 expression marks a population of adipocyte progenitors in white and brown adipose tissues. FASEB journal : official publication of the Federation of American Societies for Experimental Biology 27, 277–287. [PubMed: 23047894]

Sharp LZ, Shinoda K, Ohno H, Scheel DW, Tomoda E, Ruiz L, Hu H, Wang L, Pavlova Z, Gilsanz V, et al. (2012). Human BAT possesses molecular signatures that resemble beige/brite cells. PloS one 7, e49452. [PubMed: 23166672]

Tschop MH, Speakman JR, Arch JR, Auwerx J, Bruning JC, Chan L, Eckel RH, Farese RV, Jr., Galgani JE, Hambly C, et al. (2012). A guide to analysis of mouse energy metabolism. Nature methods 9, 57–63.

Vishvanath L, MacPherson KA, Hepler C, Wang QA, Shao M, Spurgin SB, Wang MY, Kusminski CM, Morley TS, and Gupta RK (2015). Pdgfrbeta Mural Preadipocytes Contribute to Adipocyte Hyperplasia Induced by High-Fat-Diet Feeding and Prolonged Cold Exposure in Adult Mice. Cell metabolism.

Walden TB, Hansen IR, Timmons JA, Cannon B, and Nedergaard J. (2012). Recruited vs. nonrecruited molecular signatures of brown, “brite,” and white adipose tissues. American journal of physiology Endocrinology and metabolism 302, E19–31. [PubMed: 21828341]

Wang Y, Paulo E, Wu D, Wu Y, Huang W, Chawla A, and Wang B. (2017). Adipocyte Liver Kinase b1 Suppresses Beige Adipocyte Renaissance Through Class IIa Histone Deacetylase 4. Diabetes.

Wu J, Bostrom P, Sparks LM, Ye L, Choi JH, Giang AH, Khandekar M, Virtanen KA, Nuutila P, Schaart G, et al. (2012). Beige adipocytes are a distinct type of thermogenic fat cell in mouse and human. Cell 150, 366–376. [PubMed: 22796012]

Yang Y, Smith DL, Jr., Keating KD, Allison DB, and Nagy TR (2014). Variations in body weight, food intake and body composition after long-term high-fat diet feeding in C57BL/6J mice. Obesity (Silver Spring, Md) 22, 2147–2155.

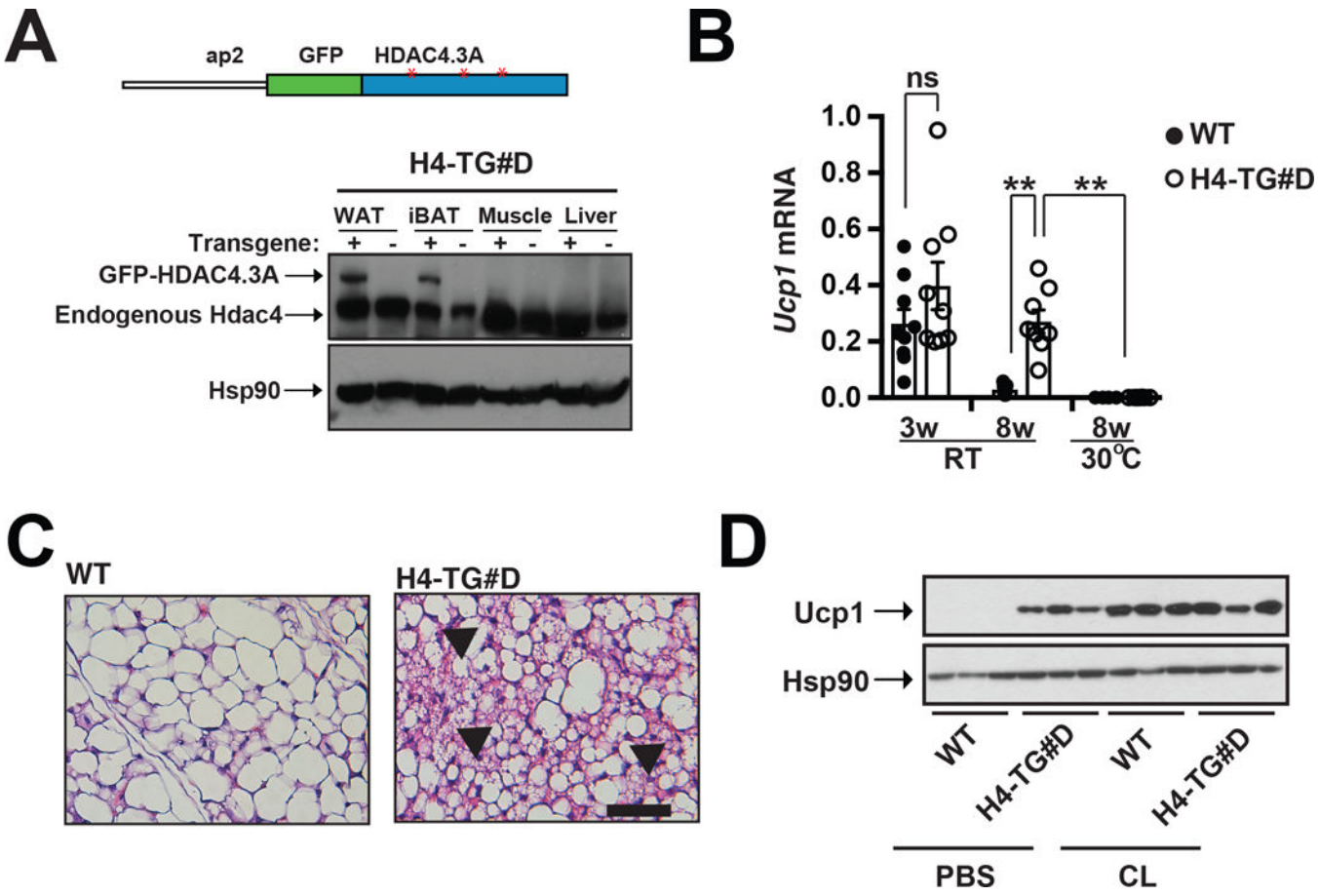

Figure 1. H4-TG mice exhibited beige adipocyte expansion in iWAT at room temperature.

A, Top: Schematic illustration of the ap2-GFP-HDAC4.3A (H4-TG) transgenic mice. ap2: fabp4 promoter; GFP: green fluorescent protein; HDAC4.3A: human HDAC4 with three SIK phosphorylation sites (Ser246, Ser467 and Ser632) Ser→Ala mutations (Red asterisks). Bottom: Immunoblot showing amounts of GFP-HDAC4.3A and Hsp90 in WAT, iBAT, muscle and liver from C57bl/6J (WT) and ap2-GFP-HDAC4.3A (H4-TG#D) mice. **B**, q-PCR analysis of *Ucp1* mRNA levels in iWAT from 3-week and 8-week-old WT and H4-TG#D mice at room temperature (RT) and 8-week-old at thermoneutrality (30ºC). Sample sizes: 3w WT/RT (n=9), 3w H4-TG#D /RT (n=9), 8w WT/RT (n=7), 8w H4-TG#D /RT (n=8), 8w WT/30ºC (n=4), and 8w H4-TG#D /30ºC (n=8). **C**, Representative H&E staining of iWAT from 8-week-old WT and H4-TG#D mice at normal chow. Scale bar: 50μM. Arrows: multilocular beige adipocytes. **D**, Immunoblots showing Ucp1 and Hsp90 in iWAT from 8-week-old WT and H4-TG#D mice treated with PBS or CL.

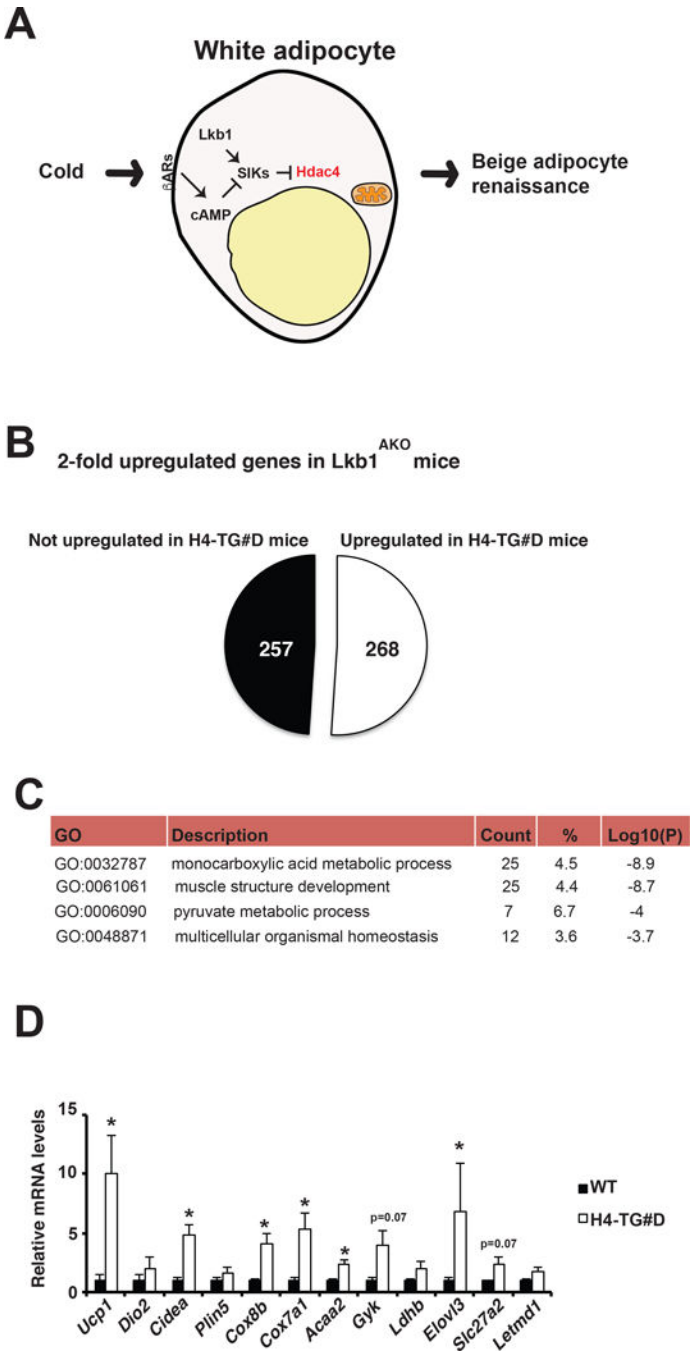

Figure 2. HDAC4 activation promoted thermogenic gene expression in iWAT.

A, Molecular mechanism of beige adipocyte renaissance. Under cold stimulation, adipocyte Hdac4 activation could promote beige adipocyte renaissance non-cell autonomously. Liver kinase b1 (Lkb1) activates Salt-inducible kinases (SIKs) to suppress Hdac4 activation, while cold stimulates Hdac4 activation through βAR-mediated inhibition of SIKs. **B**, Pie chart analysis of Hdac4 dependency of up-regulated genes identified in Lkb1^{AKO} mice. **C**, List of gene ontology (GO) number, description, count, percentage, and Log10(p) value of the top four processes enriched in Hdac4-dependent genes that were upregulated in the iWAT of

both Lkb1^{AKO} and H4-TG#D mice. **D**, q-PCR analysis of selective beige adipocyte genes in iWAT from WT and H4-TG#D mice under normal chow. Sample sizes: n=5 for each genotype.

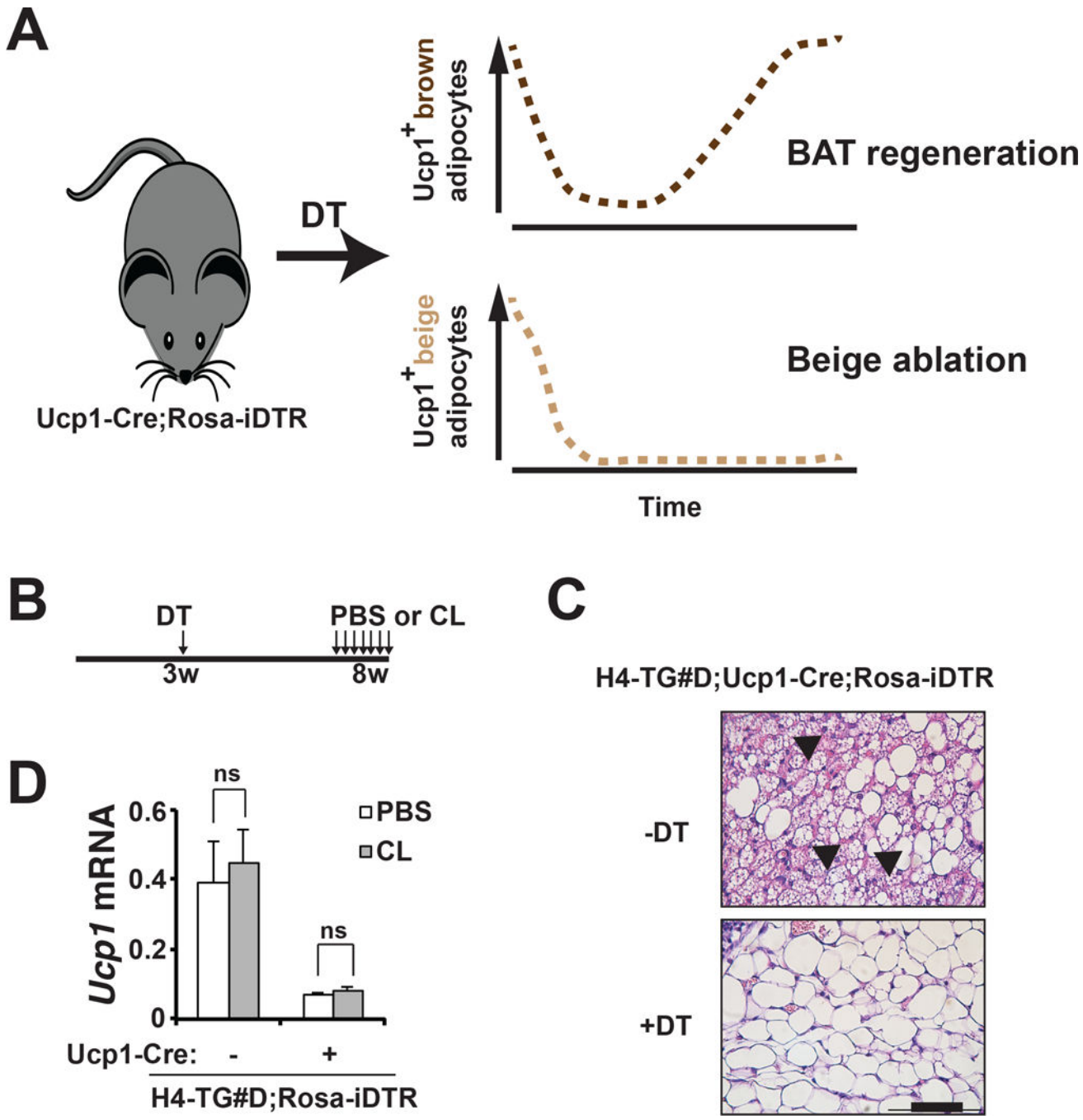

Figure 3. HDAC4 activation promoted beige adipocyte renaissance in iWAT.

A, Diagram showing beige adipocyte ablation strategy. In Ucp1-Cre;Rosa-iDTR mice at room temperature, DT injection (at three-week of age) induces cell death of Ucp1+ brown adipocytes in iBAT and beige adipocytes in iWAT within 3 days. Brown adipocytes gradually repopulate the BAT in 3–5 weeks, while Ucp1+ beige adipocytes remain absent in iWAT. **B**, Experimental design. Three-week-old H4-TG#D;Cre- (genotype: H4-TG#D;Rosa-iDTR) or H4-TG#D;Cre+ (genotype: H4-TG#D;Ucp1-Cre;Rosa-iDTR) mice were injected with DT once. Five weeks later, they were injected with either PBS or CL for 7-consective

days. **C**, Representative H&E staining of iWAT from 8-week-old H4-TG#D;Cre+ mice at normal chow, with or without DT injection at 3-week of age. Scale bar: 50μM. Arrows: multilocular beige adipocytes. **D**, q-PCR analysis of *Ucp1* mRNA levels in iWAT from ~8-week-old H4-TG#D;Cre- and H4-TG#D;Cre+ mice treated with PBS or CL. DT was injected at 3-week of age. Sample size: H4-TG#D;Cre-/PBS (n=4), H4-TG#D;Cre+/PBS (n=3), H4-TG#D;Cre-/CL (n=4) and H4-TG#D;Cre+/CL (n=5).

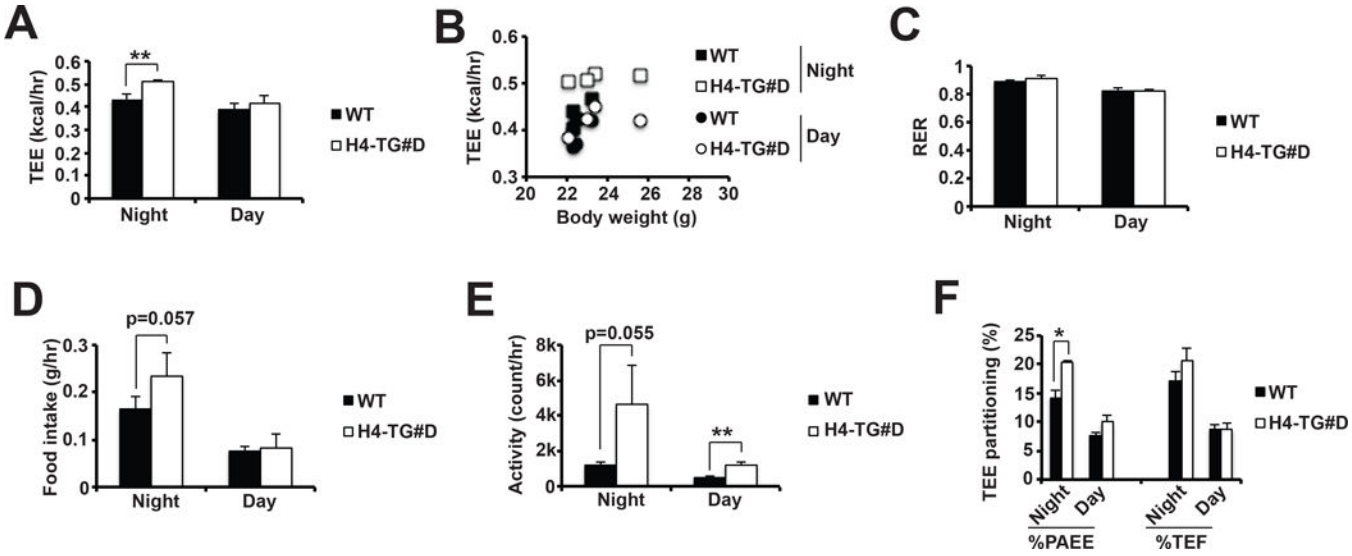

Figure 4. H4-TG mice showed increased total energy expenditure (TEE).

A, Average TEE at night and day in ~8–10-week old male WT and H4-TG#D mice at room temperature. **B**, Scatter plots of TEE at night and day over body weight in above mice. Averages of RER (**C**), food intake (**D**), and activity (**E**) at night and day in above mice. **F**, TEE partitioning of physical activity (PAEE) and food (TEF) in above mice. Sample size: n=4 for each genotype.

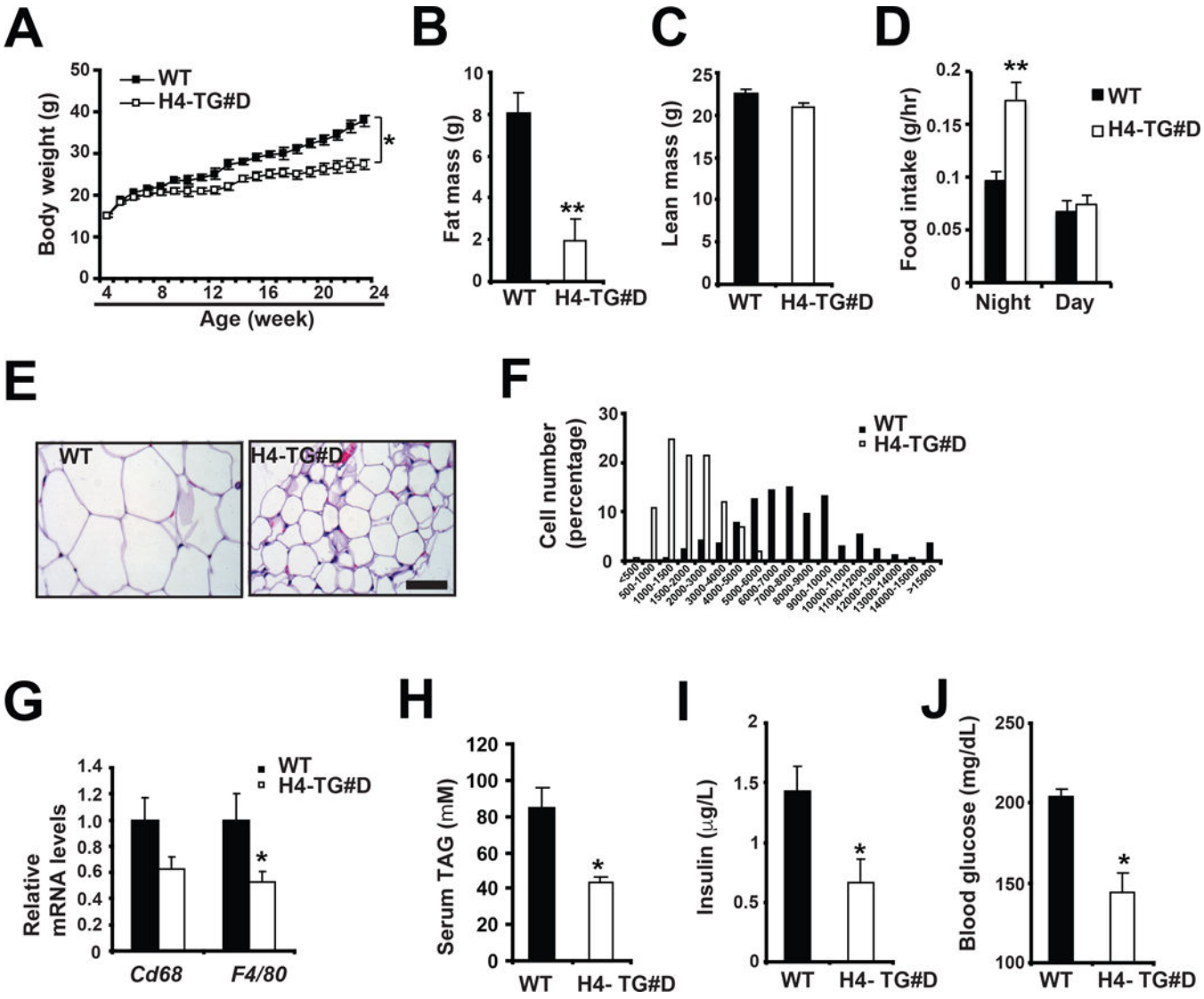

Figure 5. H4-TG mice showed reduced adiposity and improved metabolic performance under normal chow.

A, Body weight in male WT and H4-TG#D mice on normal chow. Sample sizes: n=24 for each genotype. Fat mass (**B**), lean mass (**C**) and food intake (**D**) of ~ 26-week-old WT and H4-TG#D mice. Sample sizes: n=6 for each genotype. Representative H&E staining of eWAT (**E**) and adipocyte size distribution (**F**) in above mice. Scale bar: 50μM. Total adipocytes counted: WT (n=878) and H4-TG#D (n=1319). **G**, q-PCR analysis of mRNA levels of macrophage marker *Cd68* and *F4/80* in eWAT of above mice. Serum TAG (**H**), insulin (**I**) and glucose (**J**) levels in ~ 26-week-old WT and H4-TG#D mice after 4 hour fasting. Sample sizes: n=6 for each genotype.

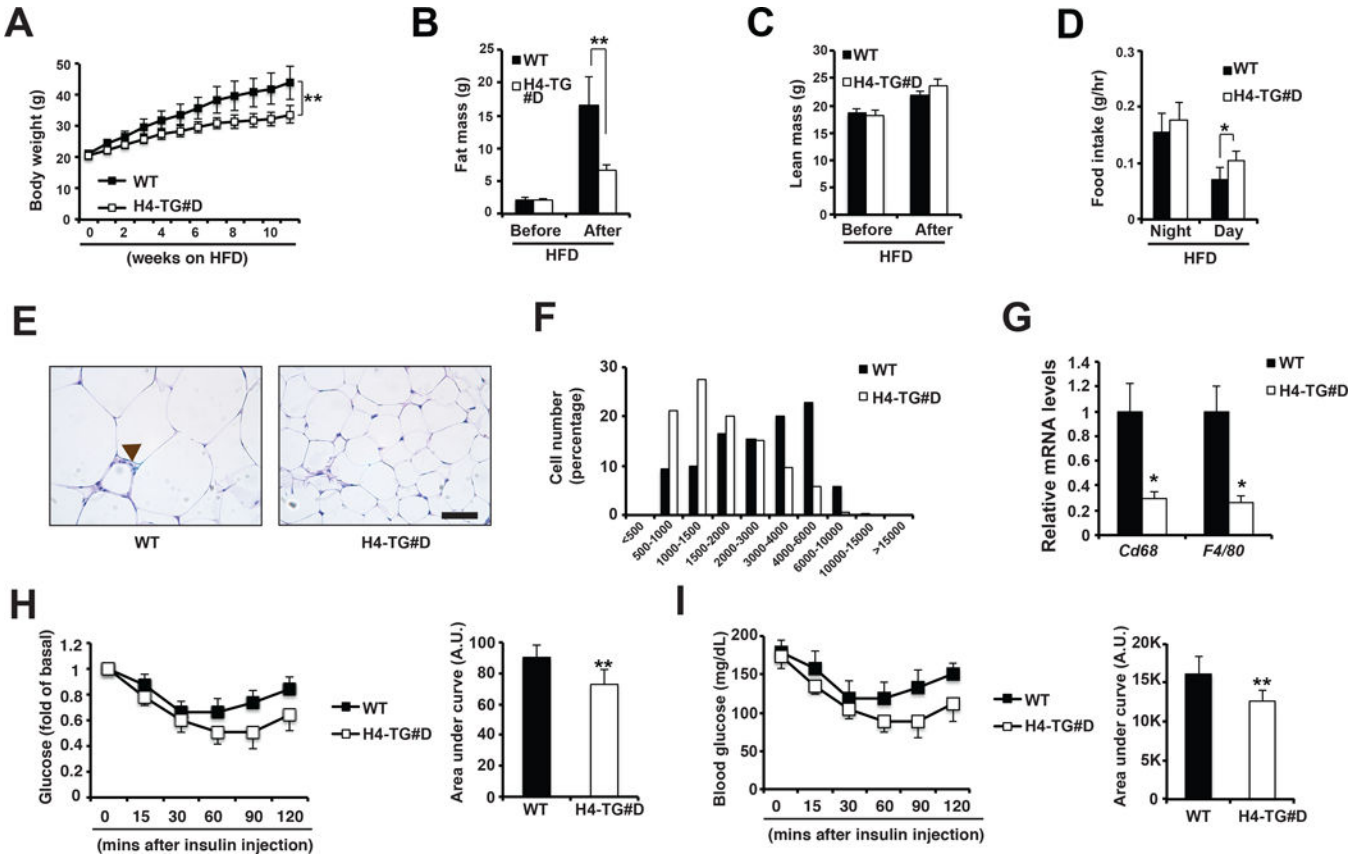

Figure 6. H4-TG mice were lean and insulin sensitive under HFD.

A, Body weight for male WT and H4-TG#D mice under ~10-week HFD. Sample sizes: WT (n=9) and H4-TG#D (n=11). Fat mass (**B**), lean mass (**C**) and food intake (**D**) of male WT and H4-TG#D mice before and after 9-week HFD. Representative H&E staining of eWAT (**E**) and adipocyte size distribution (**F**) in above mice. Scale bar: 50μM. Brown arrow: Crown-like structure. Total adipocytes counted: WT (n=2293) and H4-TG#D (n=2883). **G**, q-PCR analysis of mRNA levels of macrophage marker *Cd68* and *F4/80* in eWAT of above mice. **G**, Serum glucose levels (per fold of basal) in WT and H4-TG#D mice after 9-week HFD. AUC (area under curve) of ITT also shown. **H**, Serum glucose levels (per mg/dL) in WT and H4-TG#D mice after 9-week HFD. AUC (area under curve) of ITT also shown. A.U. Arbitrary Unit. Sample sizes: WT (n=9) and H4-TG#D (n=10).

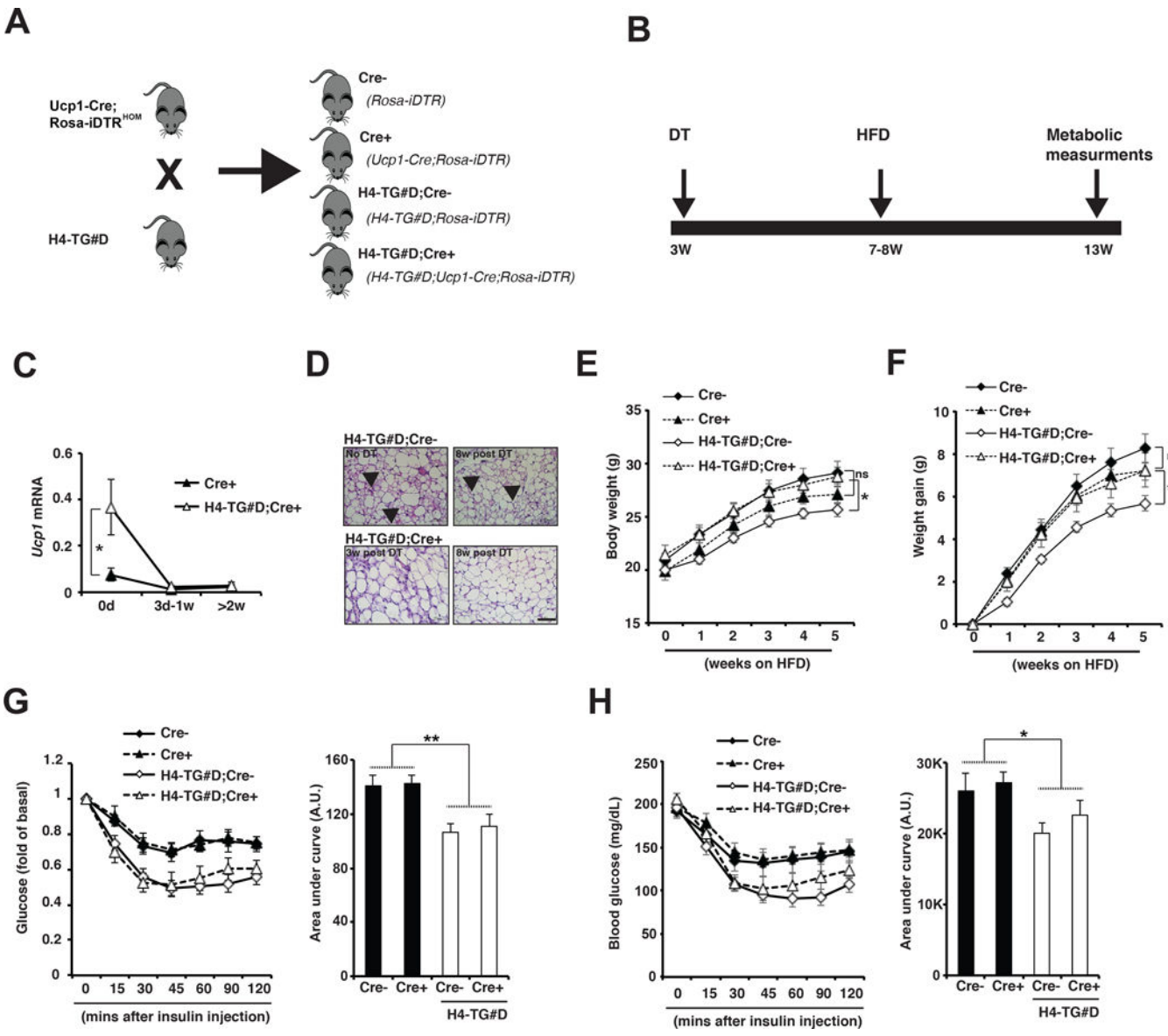

Figure 7. H4-TG mice with beige adipocyte ablation were not protected against HFD-induced obesity.

A, H4-TG#D mice were crossed to Ucp1-Cre;Rosa-iDTRHOM mice to generate the following four groups of mice: Cre- (genotype: *Rosa-iDTR*), Cre+ (genotype: *Ucp1-Cre; Rosa-iDTR*), H4-TG#D;Cre- (genotype: *H4-TG#D;Rosa-iDTR*), and H4-TG#D;Cre+ (genotype: *H4-TG#D;Ucp1-Cre;Rosa-iDTR*). **B,** Experimental scheme. The four groups of mice were injected with DT at three-week of age to ablate Ucp1+ brown and beige adipocytes. Four to five weeks later, the brown adipocytes were fully regenerated in iBAT, while beige adipocytes remained ablated in iWAT. Then the mice were fed with HFD for additional 4–5-weeks for metabolic measurements. **C**, q-PCR analysis of *Ucp1* mRNA levels in iWAT from Cre+ and H4-TG#D;Cre+ adult mice before, 3 days to 1 week, and more than 2 weeks after DT injection. Sample sizes: 0d Cre+ (n=18), 0d H4-TG#D;Cre+ (n=19), 3d-1w Cre+ (n=4), 3d-1w H4-TG#D;Cre+ (n=7), >2w Cre+ (n=5) and >2w H4-

TG;Cre+ (n=8). **D**, Representative H&E staining of iWAT from H4-TG#D;Cre- and H4-TG#D;Cre+ mice at different time-points before and after DT injection. Scale bar: 50μM. Arrows: multilocular beige adipocytes. **E, F,** Body weight and weight gain of Cre-, Cre+, H4-TG#D;Cre- and H4-TG#D;Cre+ mice under HFD. Sample sizes: Cre- (n=18), Cre+ (n=18), H4-TG#D;Cre- (n=17) and H4-TG#D;Cre+ (n=13). **G,** Serum glucose levels (per fold of basal) in Cre-, Cre+, H4-TG#D;Cre- and H4-TG#D;Cre+ mice after 5-week HFD. AUC (area under curve) of ITT also shown. **H,** Serum glucose levels (per mg/dL) in Cre-, Cre+, H4-TG#D;Cre- and H4-TG#D;Cre+ mice after 5-week HFD. AUC (area under curve) of ITT also shown. AU: Arbitrary Unit. Sample sizes: Cre- (n=18), Cre+ (n=18), H4-TG#D;Cre- (n=17) and H4-TG#D;Cre+ (n=13).